

*Received April 4, 2017; reviewed; accepted April 28, 2017*

## Kinetic separation curves based on process rate considerations

Jan Drzymala\*, Tomasz Ratajczak\*, Przemyslaw B. Kowalczyk\*\*

\* Wrocław University of Science and Technology, Faculty of Geoengineering, Mining and Geology, Wybrzeże Wyspińskiego 27, 50-370 Wrocław, Poland. Corresponding author: tomasz.ratajczak@pwr.edu.pl (Tomasz Ratajczak)

\*\* NTNU Norwegian University of Science and Technology, Department of Geoscience and Petroleum, Sem Sælands veg 1, N-7491 Trondheim, Norway

**Abstract:** There are many graphical representations of separation results involving time as a crucial parameter determining the kinetics of a process. The graphical representations of results of separation are usually in the form of 2D plots relating two parameters which one of them is time. Time can also be utilized as a complex parameter such as a process rate. The plots involving time are called kinetic curves. Theoretically, the number of kinetic curves is infinite. The basic process kinetic curves, relating either yield (or recovery) and time can be modified to obtain numerous local and global efficiency curves. The global efficiency kinetic curves provide characteristic constants which do not change with the time and yield of a process. In this paper the local and global efficiency plots were created using experimental data which followed the so-called first order kinetics. It was shown that the integral 1<sup>st</sup> order kinetic equation provided the kinetic constant  $k$  which was numerically identical with the 1<sup>st</sup> order specific rate  $v$ , while their units were different ( $k$ , 1/min;  $v$ , %/(%·min)). The global efficiency parameters plotted versus the maximum yield provided another type of plot, which can be called the limits kinetic curve. The limits kinetic curves are very useful for characterizing, quantification and classification of separation systems. The limits kinetic curves can be normalized providing one universal curve with a characteristic point, for instance,  $v_{50}$  indicating the specific rate (or kinetic) constant at the maximum recovery equal to 50%. The mathematical equation of the normalized limits kinetic curve was given in the paper.

**Keywords:** separation, flotation, kinetics, separation curve, process rate

### Introduction

An outcome of separation depends on time of a process and numerous other parameters (Wills and Napier-Munn, 2006). When the time of separation is combined with its products quantity or quality, two basic kinetic graphical plots are obtained, which can be called process and component kinetic curves, respectively. The process kinetic curve can be drawn in a form of a component recovery to concentrate versus process time, when one component of the separation system is considered, as well as

in the form of yield versus time, when all components of the feed are taken into account. In turn, the component kinetic curve relates the concentrate grade versus time of the process. The component kinetic curve, and other possible basic kinetic curves, such as for instance product name versus time, are seldom used. It can be added that some authors call the kinetic equation, used for approximation of separation data, the Boltzmann transport equations or functions (Lazic and Calic, 2000) to pay tribute to Boltzmann input to kinetics of particles at the end of XIX century. The most common flotation kinetic models are: single rate constant (Polat and Chander, 2000; Kowalczyk et al., 2016), Dirac delta function (Lynch et al., 1981; Yianatos et al., 2010), rectangular (Klimpel, 1980), Kelsall (Kelsall, 1961) and gamma (Loveday, 1966).

The basic parameters of separation processes, that is time, recovery, yield and grade, can be combined together to create new parameters (Drzymala, 2007). These parameters can be grouped into pairs containing time and plotted as kinetic efficiency curves in analogy to the upgrading efficiency curves, which do not use time as the parameter. There is an infinitive number of efficiency curves (Drzymala, 2006). The kinetics of separation can be local, when it changes with time, and global, when the efficiency is constant throughout the process. The basic and kinetic efficiency curves usually provide limits of separation in the form of maximum yield, grade and recovery. The efficiency and limit parameters can be combined, delivering the limits kinetic curves.

All the mentioned curves are presented and discussed in the paper. The limits kinetic curves can be further modified to create other relations, for instance incentive kinetic curves, relating the separation efficiency and such parameters as the particle shape, reagent dosage, pH etc. The goal of this paper is to show how different kinetic curves can be created and their properties, based preferably on the process rate, evaluated and compared.

## Process kinetic curves

The relationship between the yield and time of separation is called the process kinetic curve. This kind of plot characterizes the course of a process from the beginning to the end. Figure 1 shows two process kinetic curves, one for Hallimond tube Kupferschiefer shale flotation in the presence of hexylamine (Fig. 1a) and one for anthracite coal laboratory flotation in the presence of NaCl and sodium acetate (Fig. 1b).

The kinetic process curve does not provide explicitly additional useful information about the process such as efficiency and separation limits and relations between them. To extract these parameters from the kinetic process curve additional operations are needed leading to efficiency kinetic curves.

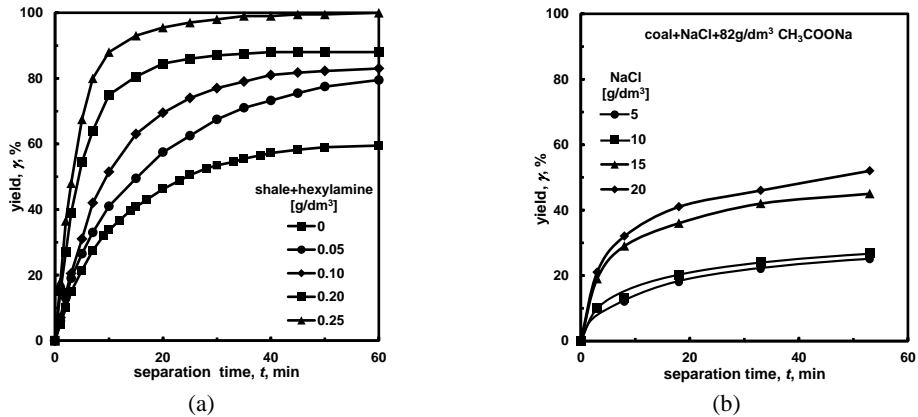


Fig. 1. Process kinetic curves in the form of yield versus time. (a) Kupferschiefer shale flotation in a 200 cm<sup>3</sup> cell, 36 cm high, Hallimond tube in the presence of hexylamine (selected data of Kudlaty, 2016), and (b) anthracite coal flotation in laboratory machine with 200 cm<sup>3</sup> cell in the presence of NaCl and 82 g/dm<sup>3</sup> of sodium acetate (selected data of Merta and Drzymala, 2016). Manual approximation of data points

## Efficiency kinetic curves

### Local efficiency kinetic curves

Combinations of the yield and time provide the efficiency of separation. When the calculated efficiency of separation changes with either time or yield of the process, such efficiency is local. The local efficiency can be once more combined with either yield or time, or both, to get still another local efficiency. In such a way unlimited number of efficiency parameters can be created. One, sometimes more, of the local efficiencies is constant, that is independent of the time and yield. Such parameter is called the global kinetic efficiency of a process.

The simplest and obvious kinetic efficiency parameter, although seldom used (Bu et al., 2017), is the rate of the process. It has a real physical and practical meaning. It is a derivative of yield in respect to time. Graphically, it is the slope of the process kinetic curve at a given moment of separation time. The simplest way of the process rate calculation is approximation of the process kinetic curve with a mathematical equation, and next calculation of the rate by differentiation. Such calculations were performed for the discussed here experimental data of Kudlaty (2016) based on shale flotation in the presence of hexylamine. Figure 2 shows approximation of the flotation kinetic data with a polynomial equation and differentiation of the obtained equation for finding and plotting the flotation rate as a function of time. Figure 2 also shows that the polynomial approximation of data points at longer time of flotation, indicated by dashed lines, is inaccurate. Therefore, the rate of flotation in this time range is also inaccurate, and therefore the polynomial approximation should be used with care.

Approximation of yield vs. time experimental data can be accomplished using other than polynomial equations. Very useful is a family of formulas:

$$\gamma = \gamma_f \left[ 1 - \frac{1}{(1+(n-1)\gamma_\infty^{n-1}pt)^{\frac{1}{1-n}}} \right] \tag{1}$$

for  $n \neq 1$ , and for  $n=1$

$$\gamma = \gamma_f [1 - \exp(-pt)] \tag{2}$$

where  $\gamma_f$  is the final yield (last data point) of the process, while  $p$  and  $n$  are constants. These formulas are based on the so-called  $n$ -order kinetic equations (Gharai and Venugopal, 2016; Bu et al., 2017). The rate of the process,  $d\gamma/dt$ , obtained by differentiation of Eqs. 1 and 2 is:

$$d\gamma/dt = (\gamma_f - \gamma)^n p. \tag{3}$$

Application of the  $n$ -order type kinetic equations with  $n=1$  for approximation of the separation data for shale flotation with  $0.1 \text{ g/dm}^3$  hexylamine is shown in Fig. 3a, while Fig 3b presents the calculated rate of the process. A comparison of Figs. 2a and 3a indicates that approximation of the considered data with  $n$ -order type for  $n=1$  kinetic equation is superior over the polynomial.

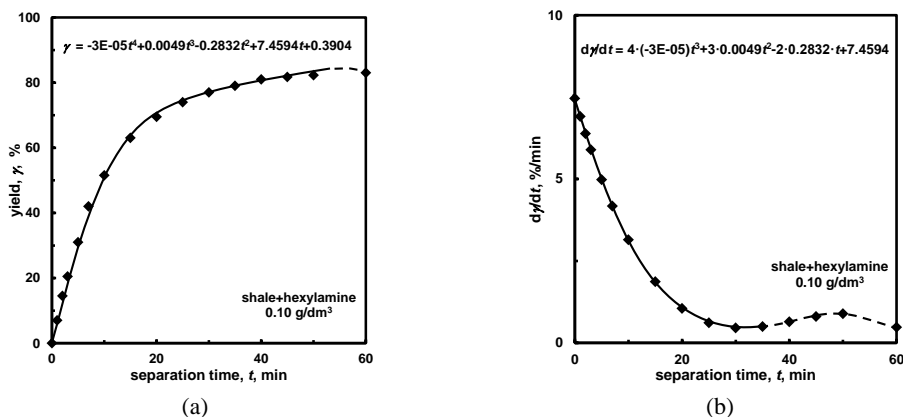


Fig. 2. Approximation of a process kinetic curve with polynomial equation (a) in order to calculate, by differentiation, and plot the local efficiency kinetic curves as the process rate vs. process time ( $d\gamma/dt$  vs.  $t$ ) (b). Hallimond tube shale flotation in the presence of  $0.10 \text{ g/cm}^3$  hexylamine (Kudlaty, 2016). Polynomial constants were determined as an average for all data points using statistics

Other equations that can be used for approximation of kinetic data and calculations of the process rate, include very likely the hyperbolic sine function, which is used for evaluation of electric charge according to the Gouy-Chapman theory (Stumm and Morgan, 1970) and has a very similar shape to the kinetic process curves.

There are other local efficiency plots based on the process rate and time. Figure 4 shows two of them, that is  $\ln(d\gamma/dt)$  vs.  $t$  (Fig. 4a) and  $(d\gamma/dt) / (\gamma_f - \gamma)^2$  vs.  $t$  (Fig. 4b).

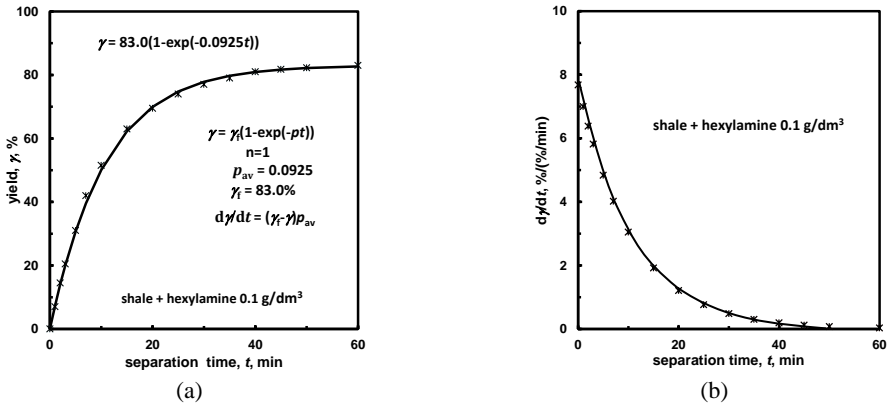


Fig. 3. Approximation of a process kinetic curve with  $n$ -order type kinetic equation for  $n=1$  (a) for calculation by differentiation and next plotting process rate  $d\gamma/dt$  as local efficiency vs. process time  $t$  (b). Replotted data from Fig. 1.  $\gamma_f$  is the last experiment data point and  $p_{av}$  was found by a trial and error method until visually the data points and approximation line were well aligned. Other approaches, including statistics and finding mean value (preferably harmonic) can also be used

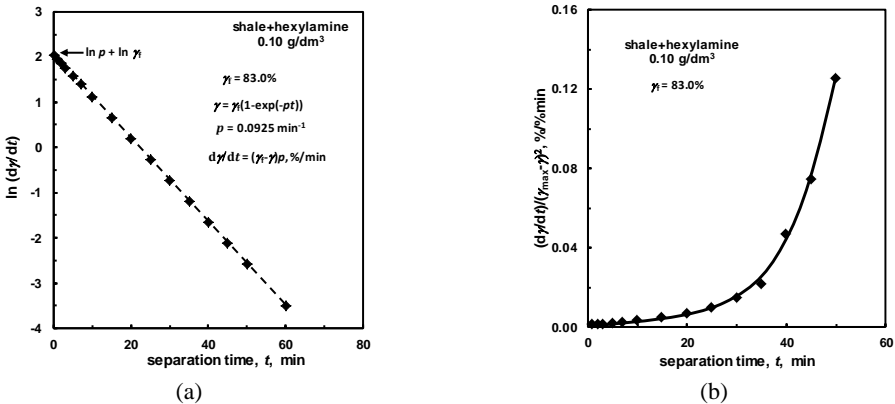


Fig. 4. Selected local efficiency kinetic curves based on the process rate  $d\gamma/dt$  (a)  $\ln(d\gamma/dt)$  vs.  $t$ , and (b)  $(d\gamma/dt)/(\gamma_f - \gamma)^2$  vs.  $t$ . Replotted data from Fig. 1

The plots shown in Fig. 4 represent local kinetic efficiencies vs. time relations because both  $\ln(d\gamma/dt)$  and  $(d\gamma/dt)/(\gamma_f - \gamma)^2$  change with time of the process. It should be noticed that the  $\ln(d\gamma/dt)$  vs. time relationship is linear. This information can be used, for instance, for comparison of different series of kinetic separation data.

Another family of local efficiencies is based on different combinations of yield  $\gamma$  and time  $t$ . As an example, Figure 5 shows two of them. The new local efficiency kinetic curves, shown in Fig. 5, do not reveal any specific information on kinetics of the process but there is always a chance that they can be used for special applications.

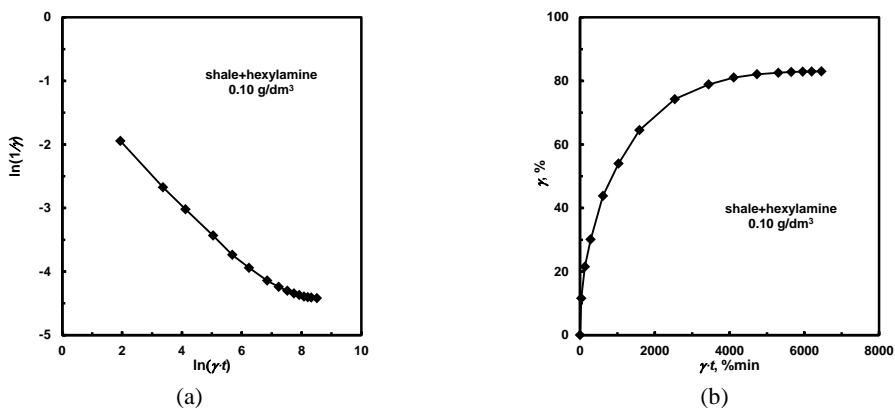


Fig. 5. Local kinetic efficiency curves based on different combinations of yield  $\gamma$  and time  $t$ , (a)  $\ln(1/\gamma)$  vs.  $\ln(\gamma t)$ , (b)  $\gamma$  vs.  $\gamma t$ . Replotted data from Fig. 1

### Global efficiency kinetic curves

The local kinetic efficiency of a separation process, to be global, must be constant regardless of the time and yield. To find the global efficiency, different mathematical formulas should be tried. In this work, during the search for the local kinetic efficiency (Figs. 2-5), it was found that the 1<sup>st</sup> order type kinetic equation, both in integral and differential forms, well matched the experimental data. It suggests that the global kinetic efficiency for the considered separation systems is the 1<sup>st</sup> order kinetic process. Different experimental data can be matched by many different kinetic orders. Some of them were reviewed elsewhere (Arbiter and Harris., 1962; Somasundaran and Lin, 1973; Ek, 1992; Hernainz and Calero, 2001; Brozek and Mlynarczykowska, 2007; Zhang et al., 2013).

Finding the global kinetic efficiency requires to determine not only the 1<sup>st</sup> order kinetic constant  $k$  but also the limit of the process  $\gamma_{\max}$ . For this purpose either integral

$$\gamma = \gamma_{\max}[1 - \exp(-kt)] \quad (4)$$

or differential

$$d\gamma/dt = (\gamma_{\max} - \gamma) \cdot v \quad (5)$$

forms of the 1<sup>st</sup> order kinetic equations can be used.

It should be noticed that  $k$ , that is the 1<sup>st</sup> order kinetic constant in Eq. 4, and the specific 1<sup>st</sup> order kinetics rate  $(d\gamma/dt)/(\gamma_{\max}-\gamma) = v$  in Eq. 5, are numerically identical. However, the unit of  $v$  is %/(%·min), while the unit of  $k$  is 1/min. This is so, because the integral equation deals only with concentrate yield ( $\gamma$ ,  $\gamma_{\max}$ ), while the differential formula takes into account amount of concentrate ( $\gamma$ ) and amount of tailing ( $\gamma_{\max}-\gamma$ ). To emphasize the fact that  $k$  and  $v$  are numerically the same, in this work the following notation will be used:  $\text{num } v = \text{num } k$ . The ways of the  $v$  and  $\gamma_{\max}$  values determination will be discussed in the following section of the paper.

## Ways of determination of global efficiency and process limits

According to numerous papers on kinetics of separation (Gharai and Venugopal, 2016; Bu et al., 2017), there are many different approaches to determine the global kinetic efficiency of a process. They are based on three elements: scattered data points, approximating equations, and a criterion of approximation, which is usually either visual matching or statistics. All approaches, as a rule, use graphs to visually check the outcome of approximation of the experimental data points. In fact all procedures are based on the trial and error method until a constant, that is global efficiency parameter, is obtained which fulfils the imposed criterion, which usually is the smallest approximation error. All the approaches are expected to provide not only the value of the global efficiency but also the limit of separation, in our case the ultimate (maximum) yield  $\gamma_{max}$ .

Plotting different local efficiency curves (Figs. 2-5) reveals that the considered in this work separation data can be characterized by a global efficiency when they are approximated with the 1<sup>st</sup> order kinetic equation, both in integral and differential forms.

The approaches used to find the global efficiency and limit of the process are based on either linear or curvilinear approximations. An example of a curvilinear approximation is given in Fig. 6. In the curvilinear approach the statistical criterion is usually the minimum value of average squared error defined as minimum value of  $\Sigma(\gamma_{calculated}-\gamma_{exp})^2/n_{exp}$ , where  $n_{exp}$  stands for the number of experimental data points. Such a procedure, or similar techniques, was applied by other authors (Li et al., 2013).

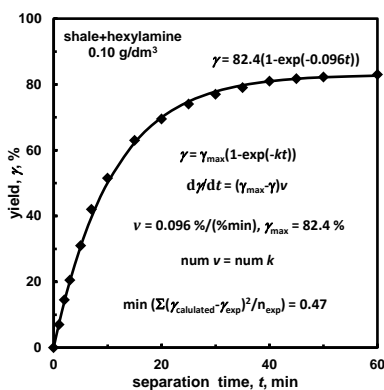


Fig. 6. Curvilinear approximation of separation data to find both global kinetic efficiency and separation limit. Approximation with the 1<sup>st</sup> order kinetic equation (Eq. 4) with two unknowns:  $k=v$  and  $\gamma_{max}$ . The approximation is based on statistical criterion that  $\Sigma(\gamma_{calculated}-\gamma_{measured})^2/n_{exp}$  is at minimum

On the other hand, the goal of the linear methods of  $k=v$  and  $\gamma_{max}$  determination is to get a straight line type relation in the efficiency plot. The direction of the straight line depends on the parameters used for plotting. Figure 7 shows three examples of such plotting. The straight line equation is a result of different possible forms of the

same 1<sup>st</sup> order kinetic equation. The possible linear forms of the 1<sup>st</sup> order kinetic equation are given in Table 1, which summarizes the calculated values of  $k$ ,  $v$  and  $\gamma_{max}$  using three linear and one curvilinear graphical methods.

It can be concluded that when the experimental data are scattered, the results of global kinetic efficiency determination depend on the method of approximation. The curvilinear method seems to be the most accurate and fast with the minimum average sum of squares of the  $(\gamma_{calculated} - \gamma_{measured})$  term as a criterion. This method provides both  $k = v$  and  $\gamma_{max}$ . The criterion used in the curvilinear approximation can be modified but no much improvement is expected. The presented here graphical methods are very useful because the outcome of approximation can be visually verified.

In this work a separation system, which follows the 1<sup>st</sup> order kinetics is considered, however, a similar procedure can be applied for any other type of separation kinetics.

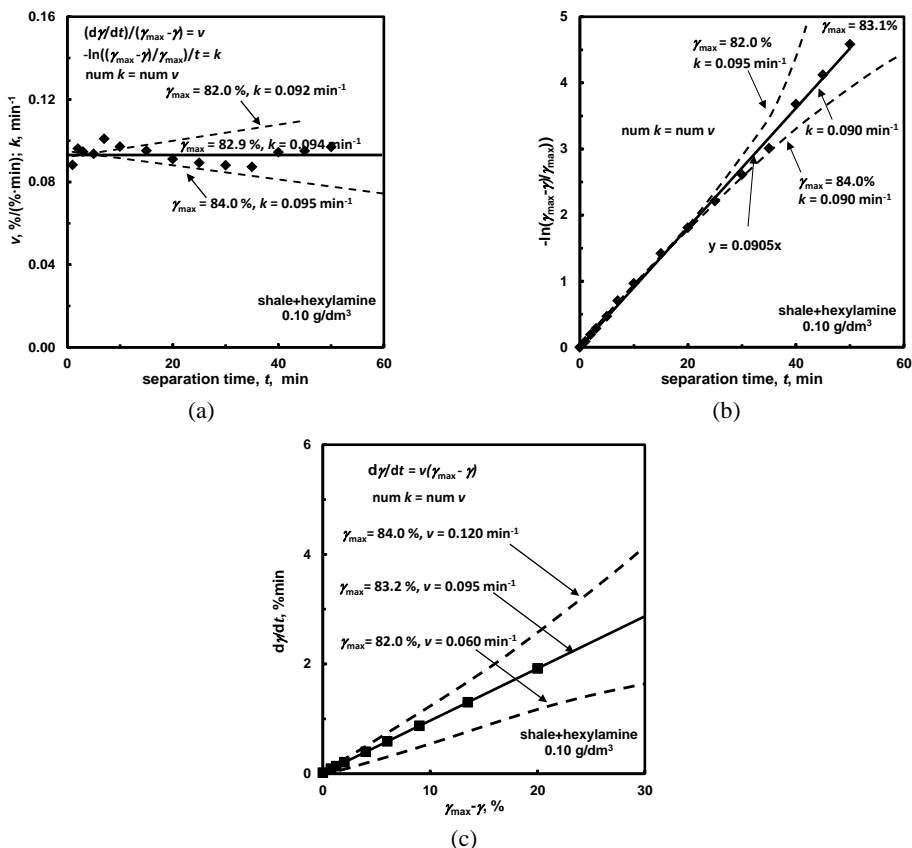


Fig. 7. Methods of graphical linear determination of global efficiency for the 1<sup>st</sup> order kinetics. Visual criterion: linear relation.  $\gamma_{max}$  is found by the trial and error method until the plot forms a straight line. The kinetic efficiency is determined from the slope of the straight line. The global kinetic efficiency is either  $k$  or  $v$  (num $v =$  num $k$ )



Table 1. Results of  $v=k$  and  $\gamma_{\max}$  determination by graphical methods. For linear determination methods criterion is linear relation,  $\gamma_{\max}$  is found by the trial and error method. The kinetic efficiency (either  $v$  or  $k$ ) is determined by the slope of the straight line ( $\text{num}v = \text{num}k$ )

Method	$\gamma_{\max}$ , %	$k$ , $\text{min}^{-1}$ , $v$ , %/ $(\% \cdot \text{min})$ ( $\text{num}v = \text{num}k$ )
Curvilinear approximation		
1 $\gamma = f(t)$ $\gamma = \gamma_{\max}(1 - \exp(-kt))$	82.4	0.096
Linear approximation		
1 $(d\gamma/dt)/(\gamma_{\max}-\gamma) = f(t)$ $(d\gamma/dt)/(\gamma_{\max}-\gamma) = v$ or $-\ln((\gamma_{\max}-\gamma)/\gamma_{\max})/t = k$ plot type $y=\text{const}$ , slope zero	82.9	0.094
2 $-\ln(\gamma_{\max}-\gamma)/\gamma_{\max}) = f(t)$ $-\ln((\gamma_{\max}-\gamma)/\gamma_{\max}) = kt$ plot type $y=ax$ , slope $a = k$	83.1	0.090
3 $d\gamma/dt = f(\gamma_{\max}-\gamma)$ $d\gamma/dt = v(\gamma_{\max}-\gamma)$ plot type $y=ax$ , slope $a = v$	83.2	0.095

### Limits kinetic curves

The specific rates and maximum (ultimate) yields  $\gamma_{\max}$  can be used for plotting another useful kinetic relation, that is the limits kinetic curves (Chipfunhu et al., 2012). Figure 8 presents the calculated values of  $\gamma_{\max}$  and specific 1<sup>st</sup> order rate  $v$  (numerically equal to 1<sup>st</sup> order kinetic constant  $k$ ) for the considered here flotation data of coal and shale.

The limits kinetic plot is a good base for classification of separation processes into fast-powerful, fast-powerless, slow-powerful and slow-powerless. According to such classification, flotation of coal in the presence of varying amount of NaCl and constant concentration of sodium acetate is a slow and powerless process, while flotation of shale in the presence of increasing amount of hexylamine is a powerful and slow process.

The limits kinetic curve can also be used for characterization and comparing different separation processes. For this purpose it is convenient to normalize the specific rates taking into account the value of the specific rate corresponding to the ultimate yield equal to 50% ( $k_{50}$ ,  $v_{50}$ ,  $\text{num}k_{50} = \text{num}v_{50}$ ). The 50% reference point is very convenient from theoretical and mathematical point of view because it provides the smallest scattering of the experimental data being compared after normalization. However, from practical point of view the choice of yield or recovery equal to 75%, or even higher, as the reference point, can also be used because separation, in most cases, is performed to obtain as high as possible material or component removal.

Figure 9 presents the considered here two series of separations as well as another literature data. Only data which follow the first order kinetic equation were used because only the same type of specific rate ( $v$ ) or kinetic constant ( $k$ ) can be used for comparison.

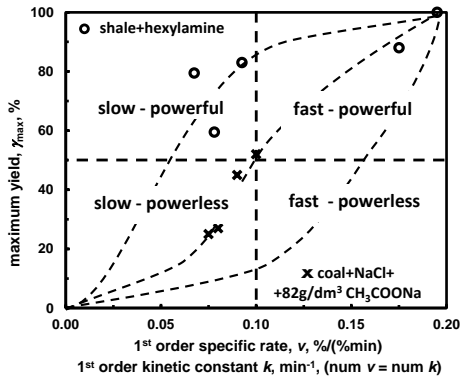


Fig. 8. Limits kinetic curves for the considered in this work separation processes which follow 1<sup>st</sup> order kinetics

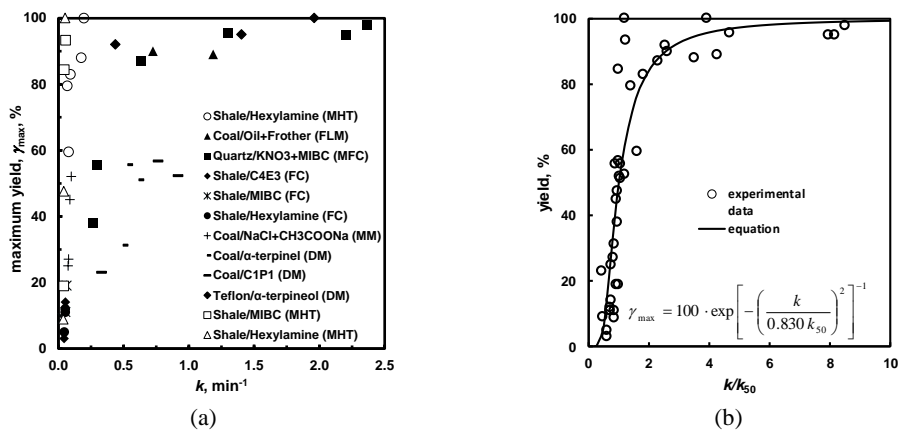


Fig. 9. (a) Limits kinetic curves, and (b) universal limits kinetic curves after normalization against kinetic constant for maximum yield of 50%. Note that  $numk_{50} = numv_{50}$  and  $numk = numv$

It can be seen from Fig. 9 that all the experimental series tend to assume a similar shape with the exception of the high values of maximum yield  $\gamma_{max}$ , probably due to a kinetic border imposed by the separation device. The normalized limits kinetic curves seem to follow the empirical equation

$$\gamma_{max} = 100 \cdot \exp \left[ - \left( \frac{k}{0.830 k_{50}} \right)^2 \right]^{-1} \tag{6}$$

where  $k_{50}$  is the 1<sup>st</sup> order kinetic constant (numerically equal to 1<sup>st</sup> order kinetic process rate  $v_{50}$ ) at maximum yield of 50%, while 0.830 is a normalization parameter

which makes  $\gamma_{\max}=50\%$  at  $k=k_{50}$ . Table 2 shows the  $k_{50}$  values for the separation systems considered in Fig. 9.

Table 2, for instance, indicates that from the kinetic point of view, flotation of shale in the presence of hexylamine is much less efficient than that of coal with di(propylene glycol) methyl ether, because the 1<sup>st</sup> order kinetic constant of the first process at  $\gamma_{\max}$  50% is  $0.050 \text{ min}^{-1}$ , while for the latter  $0.770 \text{ min}^{-1}$ . It should be kept in mind that  $\text{num } k_{50} = \text{num } v_{50}$  and  $\text{num } k = \text{num } v$ , and that the unit of  $k$  is  $\text{min}^{-1}$ , while that of  $v$  is  $\% / (\% \cdot \text{min})$ .

Table 2. The  $k_{50}$  values for different separation systems. Symbols in the bracket denote the type of flotation device: MHT- monobubble Hallimond tube, MM- Mechanobr type laboratory machine, FC- flotation column, DM- Denver type laboratory machine, LFM- laboratory flotation machine, MFC- mechanical flotation cell. MIBC-methyl isobutyl carbinol, C<sub>4</sub>E<sub>3</sub>- tri(ethylene glycol) butyl ether, C<sub>1</sub>P<sub>2</sub>- di(propylene glycol) methyl ether.

No.	Separation system	$k_{50}, \text{min}^{-1}$
1	Shale/MIBC (MHT) <sup>a</sup>	0.045
2	Shale/Hexylamine (MHT) <sup>a</sup>	0.046
3	Shale/Hexylamine (MHT) <sup>b</sup>	0.050
4	Shale/MIBC (FC) <sup>c</sup>	0.064
5	Shale/C <sub>4</sub> E <sub>3</sub> (FC) <sup>c</sup>	0.076
6	Shale/Hexylamine (FC) <sup>c</sup>	0.076
7	Coal/NaCl+CH <sub>3</sub> COONa (MM) <sup>d</sup>	0.100
8	Teflon/ $\alpha$ -terpineol (DM) <sup>e</sup>	0.173
9	Coal/oil+frother (FLM) <sup>f</sup>	0.278
10	Quartz/KNO <sub>3</sub> +MIBC (MFC) <sup>g</sup>	0.278
11	Coal/ $\alpha$ -terpineol (DM) <sup>h</sup>	0.597
12	Coal/C <sub>1</sub> P <sub>2</sub> (DM) <sup>h</sup>	0.770

Data of: a - Szajowska et al. (2014), b - Kudlaty et al. (2016), c - Kowalczyk et al. (2015),  
d - Merta and Drzymala (2016), e - Kowalczyk and Zawala (2016), f - Kalinowski and Kaula (2013),  
g - Chipfunhu et al. (2012), h - Janicki et al. (2015)

## Conclusions

The separation kinetic curves can be very useful not only for characterizing separation processes but also for their classification as well as comparison of different separation results. Since there is theoretically infinite number of separation kinetic curves, the most useful should be properly named and classified. Basing on literature kinetic data, the local and global efficiency of the process as well as limits kinetic curves were presented and discussed. The importance of process rate and specific process rates representing real and measurable process parameters, in contrast to numerous kinetic constants, were emphasized.

## Acknowledgements

The work was financed by the Polish Statutory Research Grant (No. 0401/0124/16). The author would like to thank Mr. Tomasz Kudlaty for permission to use his experimental data extracted from the BSc thesis. Thanks are due to Mr. Jakub Obuchowski for his curvilinear suggestions and calculations..

## Reference

- ARBITER, N., HARRIS, C.C., 1962. *Flotation kinetics*. In: Froth flotation: 50th anniversary volume. Fuerstenau D. (Ed.), American Institute of Mining, Metallurgical and Petroleum Engineers, New York.
- BROZEK, M., MLYNARCZYKOWSKA, A., 2007. *Analysis of kinetics models of batch flotation*. Physicochem. Probl. Miner. Process., 41, 51-65.
- BU, X. XIE, G, PENG, Y., GE, L., NI, C, 2017. *Kinetics of flotation. Order of process, rate constant distribution and ultimate recovery*. Physicochem. Probl. Miner. Process., 53(1), 342-365.
- CHIPFUNHU, D., ZANINA, M., GRANO, S., 2012. *Flotation behaviour of fine particles with respect to contact angle*. Chem. Eng. Res. Des., 90, 26-32.
- DRZYMALA, J., 2006, *Atlas of upgrading curves used in separation and mineral science and technology*. Physicochem. Probl. Miner. Process., 40, 19-29.
- DRZYMALA, J., 2007. *Mineral Processing. Foundations of theory and practice of mineralurgy*. Oficyna Wyd. PWr., Wrocław.
- EK, C., 1992. *Flotation kinetics*. In: Innovations in Flotation Technology (Mavros P., Matis K.A. Eds.). Kluwer Academic Publisher.
- GHARAI, M., VENUGOPAL, R., 2016. *Modeling of flotation process – an overview of different approaches*. Miner. Process Extr. Metall. Rev., 37(2), 120-133.
- HERNAINZ, F., CALERO, M., 2001. *Froth flotation: kinetic models based on chemical analogy*. Chem. Eng. Process., 40, 269-275.
- JANICKI, M., BARTKOWICZ, L., ZAKRECKI, B., KOWALCZYK, P.B., 2015. *Collectorless coal flotation in the presence of foaming agents*. III Polish Mining Congress, Mineralurgy and Utilization of Mineral Resources, Drzymala J., P. B. Kowalczyk (Ed.), 14-16 September, Wrocław, 52-60 (in Polish), doi: 10.5277/mineralurgia1510.
- KALINOWSKI, K., KAULA, R., 2013. *Verification of flotation kinetics model for triangular distribution of density function of floatabilities of coal particles*. Arch. Min. Sci., 58(4) 1279-1287.
- KELSALL, D.F., 1961. *Application of probability in the assessment of flotation systems*. Trans. Inst. Min. Metall., 70, 191-204.
- KLIMPEL, R.R., 1980. *Selection of chemical reagents for flotation*. In: Mular A., Bhappu R. (Eds.), Mineral Processing Plant Design, 2nd Ed. SME, Littleton, CO., pp 907-934.
- KOWALCZYK, B.P, ZAWALA, J., 2016. *A relation between time of the three –phase contact formation and flotation kinetics of naturally hydrophobic solids*. Colloids and Surfaces A., Phys. Eng. Aspects, 506, 371-377.
- KOWALCZYK P.B., ZAWALA J., KOSIOR D., DRZYMALA J., MALYSA K., 2016. *Three-phase contact formation and flotation of highly hydrophobic polytetrafluoroethylene in the presence of increased dose of frothers*. Ind. Eng. Chem. Res. 55(3), 839-843.
- KOWALCZYK, P. B., MROCZKO, D., DRZYMALA, J., 2015. *Influence of frother type and dose on collectorless flotation of copper-bearing shale in a flotation column*. Physicochem. Probl. Miner. Process., 51(2), 547-558.

- KUDLATY, T., 2016. *Maximum size of floating particles of copper-bearing shale in the presence of frothers*. BSc thesis (P.B. Kowalczyk-supervisor), Wrocław University of Science and Technology, Wrocław, Poland (in Polish).
- LAZIC, P., CALIC, N., 2000. *Boltzmann's model of flotation kinetics*. Proc. XXI IMPC (Rome), vol. B, 87-93.
- LI, Y., ZHAO, W., GUI, X., ZHANG, X., 2013. *Flotation kinetics and separation selectivity of coal size fractions*. Physicochem. Probl. Miner. Process., 49(2), 387-395
- LOVEDAY, B.K., 1966. *Analysis of froth flotation kinetics*. Trans. Am. Soc. Min. Metal. Eng., C219-C225.
- LYNCH, A.J., JOHNSON, N.W., MANLAPIG, E.V., THORNE C.G., 1981. *Mineral and coal flotation circuits*. Elsevier Scientific Publishing Co., Amsterdam.
- MERTA, P., DRZYMALA, J., 2016. *Influence of sodium chloride and sodium acetate on flotation of anthracite coal as a model substance rich in kerogen*. In Kupferschiefer II, Kowalczyk P. B., Drzymala J. (Eds.), WGGG, Wrocław, 195-200 (in Polish), doi: 10.5277/lupek1632.
- POLAT, M., CHANDER, S., 2000. *First-order flotation kinetics models and methods for estimation of true distribution of flotation rate constants*. Int. J. Miner. Process., 58, 145-166.
- SOMASUNDARAN, P., LIN, I.J., 1973. *Method for evaluating flotation kinetics parameters*. Transactions of SME, 254, 181-184
- STUMM, W., MORGAN, J.J., 1970. *Aquatic chemistry, an introduction emphasizing chemical equilibria in natural waters*. Wiley, New York.
- SZAJOWSKA, J., WEJMAN, K., KOWALCZUK, P. B., 2014. *Froth flotation of shale and quartz the in Hallimonda tube*. In Kupferschiefer, Kowalczyk P. B., Drzymala J. (Eds.), WGGG, Wrocław, 91-97 (in Polish), doi: 10.5277/lupek1417.
- WILLS, B., NAPIER MUNN, T., 2006. *Wills' mineral processing technology. An introduction to the practical aspects of ore treatment and mineral recovery*. 7th ed., Butterworth-Heinemann, London.
- YIANATOS, J., BERGH, L., VINNETT, L., CONTRERAS, F., DIAZ, F., 2010. *Flotation rate distribution in the collection zone of industrial cells*. Miner. Eng., 23, 1030-1035.
- ZHANG, H., LIU, J., CAO, Y., WANG, Y., 2013. *Effects of particle size on lignite reverse flotation kinetics in the presence of sodium chloride*. Powder Technol., 246, 658-663.